EUKARYOTIC CELL, Feb. 2011, p. 237–248 Vol. 10, No. 2
1535-9778/11/$12.00 doi:10.1128/EC.00194-10
Copyright © 2011, American Society for Microbiology. All Rights Reserved.

Involvement of an Alternative Oxidase in Oxidative Stress and Mycelium-to-Yeast Differentiation in *Paracoccidioides brasiliensis*▽†

Vicente P. Martins,[1]‡ Taisa M. Dinamarco,[1] Frederico M. Soriani,[1]‡ Valéria G. Tudella,[1] Sergio C. Oliveira,[5] Gustavo H. Goldman,[2,4] Carlos Curti,[3] and Sérgio A. Uyemura[1]*

Departamento de Análises Clínicas, Toxicológicas e Bromatológicas,[1] Departamento de Ciências Farmacêuticas,[2] and Departamento de Física e Química,[3] Faculdade de Ciências Farmacêuticas de Ribeirão Preto, Universidade de São Paulo, Ribeirão Preto, São Paulo, Brazil; Laboratório Nacional de Ciência e Tecnologia do Bioetanol (CTBE), São Paulo, Brazil[4]; and Departamento de Bioquímica e Imunologia, Instituto de Ciências Biológicas, Universidade Federal de Minas Gerais, Belo Horizonte, Minas Gerais, Brazil[5]

Received 7 August 2010/Accepted 10 December 2010

***Paracoccidioides brasiliensis* is a thermodimorphic human pathogenic fungus that causes paracoccidioidomycosis (PCM), which is the most prevalent systemic mycosis in Latin America. Differentiation from the mycelial to the yeast form (M-to-Y) is an essential step for the establishment of PCM. We evaluated the involvement of mitochondria and intracellular oxidative stress in M-to-Y differentiation. M-to-Y transition was delayed by the inhibition of mitochondrial complexes III and IV or alternative oxidase (AOX) and was blocked by the association of AOX with complex III or IV inhibitors. The expression of *P. brasiliensis aox* (*Pbaox*) was developmentally regulated through M-to-Y differentiation, wherein the highest levels were achieved in the first 24 h and during the yeast exponential growth phase; *Pbaox* was upregulated by oxidative stress. *Pbaox* was cloned, and its heterologous expression conferred cyanide-resistant respiration in *Saccharomyces cerevisiae* and *Escherichia coli* and reduced oxidative stress in *S. cerevisiae* cells. These results reinforce the role of *Pb*AOX in intracellular redox balancing and demonstrate its involvement, as well as that of other components of the mitochondrial respiratory chain complexes, in the early stages of the M-to-Y differentiation of *P. brasiliensis*.**

Paracoccidioides brasiliensis, which is a thermally dimorphic fungus, is the etiological agent of paracoccidioidomycosis (PCM), which is the most prevalent human systemic mycosis in Latin America (5, 52) and affects almost 10 million individuals in Latin America (54). It is acquired by the inhalation of airborne microconidia, which reach the pulmonary alveolar epithelium and transform into the pathogenic yeast form (52, 54, 59). The human form of PCM that is caused by this fungus is characterized by a range of clinical manifestations, ranging from asymptomatic forms to severe, disseminated, and often fatal disease. Usually, fibrosis sequelae in the affected organs may interfere with the well-being of the patient (50).

During infection, thermodimorphic fungi, such as *Histoplasma capsulatum*, *Blastomyces dermatitidis*, and *P. brasiliensis*, differentiate from a mycelial into a pathogenic yeast form, a transition that can also be induced (*in vitro*) by temperature changes from between 23 and 26°C to between 35 and 37°C. In addition, these pathogens are often subjected to significant environmental stresses, including exposure to the reactive oxygen species (ROS) and reactive nitrogen species (RNS) that are produced by the host cells (6, 27, 45).

Elevated sublethal temperatures (thermal stress or heat shock) increase ROS generation and oxidative damage in a variety of eukaryotic cells (16, 49, 60, 73). Mitochondria are the primary intracellular sources of ROS, which are generated in respiratory chain complexes I and III and can damage biomolecules, such as nucleic acids, lipids, and proteins (20–22). In order to control ROS levels, cells employ diverse detoxification mechanisms, including superoxide dismutase, catalase, the glutathione/thioredoxin system (15), and uncoupling proteins (26).

In addition to proton-pumping complexes, the mitochondrial respiratory chains of plants and fungi possess alternative pathways, which are primarily alternative NADH-ubiquinone oxidoreductases and alternative ubiquinol oxidases (cyanide-resistant oxidases) that reportedly prevent ROS generation (28, 35). We have previously demonstrated the presence of both activities in the mitochondrial respiratory chain of *P. brasiliensis* yeast cells, as well as the presence of whole (complex I to V) and functional respiratory chains (40). Here, we addressed respiratory chain complexes and alternative pathways, as well as oxidative stress, in the mycelium-to-yeast (M-to-Y) differentiation of the fungus. Moreover, we cloned alternative oxidase (AOX) and heterologously expressed *P. brasiliensis aox* (*Pbaox*) in *Escherichia coli* and *Saccharomyces cerevisiae*. We found that AOX and other respiratory chain complexes are closely involved in the early stages of the M-to-Y differentiation of *P. brasiliensis*.

* Corresponding author. Mailing address: Departamento de Análises Clínicas, Toxicológicas e Bromatológicas, Faculdade de Ciências Farmacêuticas de Ribeirão Preto, Universidade de São Paulo, Av. Café, s/n, 14040-903 Ribeirão Preto, São Paulo, Brazil. Phone: 55-016-3602-1471. Fax: 55-016-3602-4725. E-mail: suyemura@fcfrp.usp.br.

† Supplemental material for this article may be found at http://ec.asm.org/.

‡ Present address: Departamento de Bioquímica e Imunologia. Instituto de Ciências Biológicas, Universidade Federal de Minas Gerais, Av. Antonio Carlos, 6627, 31270-901 Belo Horizonte, Minas Gerais, Brazil.

▽ Published ahead of print on 23 December 2010.

MATERIALS AND METHODS

Chemicals. Antimycin A (Ant A), benzohydroxamic acid (BHAM), bovine serum albumin (BSA), dimethyl sulfoxide (DMSO), dithiothreitol (DTT), EGTA, 3-(4,5-dimethylthiazol-2-yl)-2,5-diphenyltetrazolium bromide (MTT), flavone, potassium cyanide (KCN), rotenone, salicylhydroxamic acid (SHAM), and menadione were purchased from Sigma (St. Louis, MO). Hydrogen peroxide (H_2O_2), sodium nitroprusside (SNP), and absolute ethanol were purchased from Merck (Darmstadt, Germany). All other reagents were of analytical grade. All aqueous stock solutions were prepared using glass-distilled deionized water, except for water-insoluble compounds, which were prepared in DMSO or absolute ethanol.

Strains and culture conditions. *P. brasiliensis* isolate 18 was maintained in the mycelial form in a solid Sabouraud medium (BD, NJ) at room temperature and in the yeast form in a solid PGY medium (0.5% [wt/vol] peptone, 1% [wt/vol] glucose, 0.5% [wt/vol] yeast extract, and 1.7% [wt/vol] agar) at 35.5°C. The routine cultivation of *P. brasiliensis* yeast cells was performed in liquid PGY medium (complete medium) under rotary shaker aeration at 35.5°C (58). In some experiments of M-to-Y differentiation, the fungus was grown in a liquid minimum medium (53) that had been supplemented with 0.2 g/liter L-cystine, 0.1 g/liter methionine, and 0.1 g/liter cysteine.

S. cerevisiae yeast strain INVSc1 (Invitrogen) was grown in a Sc-URA$^-$ medium (0.67% [wt/vol] yeast nitrogen base without amino acids, 2% [wt/vol] glucose or galactose [fermentable medium], or 2% [vol/vol] glycerol/ethanol [nonfermentable medium]) with amino acids or nitrogen bases as required.

E. coli Rosetta(DE3)pLysS and DH5-α were grown in a Luria-Bertani (LB) medium that had been supplemented with the required antibiotics according to the specific plasmids.

***P. brasiliensis* spheroplast preparation.** The spheroplasts of *P. brasiliensis* were produced from yeast cells in the exponential (72- to 96-h) growth stage. Cells were harvested by the centrifugation of 150 ml of culture medium, washed with a cold phosphate buffer solution (PBS), and preincubated for 1 h at 37°C with shaking at 100 rpm in a medium that contained 0.7 M sucrose, 30 mM DTT, and 100 mM Tris-HCl at a pH of 6.5. After this pretreatment, the cells were harvested and washed twice with a digestion buffer that contained 0.7 mM sucrose and 50 mM Tris-HCl at a pH of 6.5. The digestion of the yeast cell wall was accomplished by incubation in 10 ml of digestion buffer that contained 35 mg of Glucanex (Novo Nordisk, Denmark) per gram of wet cells for 5 h at 37°C with shaking at 100 rpm. The digestion was stopped by the addition of an equal volume of cold digestion buffer, and the spheroplasts were washed twice with the same buffer. The suspension was centrifuged in a swing bucket rotor (Eppendorf centrifuge model 5810 R) at 2,000 × *g* for 10 min at 4°C, and the spheroplasts were maintained on ice until use.

***S. cerevisiae* spheroplast preparation and mitochondrial isolation.** *S. cerevisiae* spheroplast preparation and mitochondrial isolation were performed according to the method of Magnani et al. (35). Cells were harvested by the centrifugation of exponentially growing cultures (30 h), washed twice in sterile water, resuspended in 10 mM Tris-HCl at a pH of 8.5 and 100 mM β-mercaptoethanol, and incubated for 10 min at 30°C. The cells were washed twice with sterile water and once with digestion buffer (1.3 M sorbitol, 10 mM imidazole-HCl at a pH of 6.4, 0.5 mM EDTA, and 0.2% BSA [wt/vol]). The spheroplasts were formed by enzymatic digestion with zymolyase 20T (Seikagatsu Corp.) at 33°C for 30 min. The spheroplasts were harvested, washed with digestion buffer, and gently homogenized in a resuspension buffer (0.3 M sorbitol, 10 mm imidazole-HCl at a pH of 6.4, 0.5 mM EDTA, and 0.2% BSA [wt/vol]). The spheroplasts were then used for experiments or lysed for mitochondrial isolation using an Elvehjem-Potter homogenizer with the addition of a protease inhibitor cocktail (Sigma) and 1 mM phenylmethanesulfonyl fluoride (PMSF). The homogenate was centrifuged at 2,000 × *g* for 5 min at 4°C. The supernatant was collected and centrifuged at 18,000 × *g* for 20 min at 4°C. Mitochondrial pellets were resuspended gently with a mitochondrial buffer (0.6 M mannitol, 10 mm Tris-HCl at a pH of 6.4, and 0.5 mM EGTA) and centrifuged once more at 2,000 × *g* for 5 min at 4°C in order to remove possible cell debris contaminants. A final centrifugation of the supernatant was performed as described above, and the mitochondrial pellet was resuspended in a mitochondrial buffer. The protein concentration was determined by the Biuret assay using BSA as standard (18).

M-to-Y differentiation of *P. brasiliensis* in complete and minimum media. *P. brasiliensis* yeast cells were initially grown to the mid-exponential growth phase in a liquid PGY medium at 35.5°C. Cells were harvested by centrifugation, washed twice using fresh medium, and then incubated for 10 days at 26°C in order to obtain *P. brasiliensis* mycelia. Mycelial cells were harvested, washed twice in sterile water, inoculated in liquid PGY or minimum medium, and incubated at 35.5°C for 10 days (12). Aliquots were collected at 0, 10, 24, 48, 72, 120, and 240 h after the temperature was shifted (26°C to 35.5°C) for visual analyses or were processed for RNA isolation and real-time PCR. Dimorphic transition was quantified by counting the different morphotypes that are produced during this process in accordance with parameters previously described (12, 48). Fungal clumps were broken by vortexing and up/down pipetting and then analyzed under the microscope.

M-to-Y differentiation of *P. brasiliensis* in the presence of mitochondrial respiratory chain inhibitors. *P. brasiliensis* mycelial cells were differentiated into yeast cells, as described above. Cells were divided into different flasks, and mitochondrial respiratory chain inhibitors were added to the cultures at time zero at the following concentrations: 2 mM SHAM, 1 mM KCN, 1.8 μM antimycin A, 2 mM BHAM, 500 μM flavone, and 20 μM rotenone. In some flasks, compounds were added in combinations, such as KCN-SHAM, antimycin A-SHAM, and rotenone-SHAM. DMSO and ethanol were also tested in order to determine the possible effects of these solvents on fungal differentiation. The addition of compounds that showed no effect on fungal differentiation was repeated after 24 or 72 h to rule out the possibility of drug degradation. Aliquots were collected at 24, 48, 72, 120, and 240 h, and images were captured using a 40× objective lens, resulting in a final magnification of ×400, using an Olympus BX51 model U-LH100-3 microscope (Tokyo, Japan) coupled to an Olympus model C-5060 wide-zoom digital camera (Tokyo, Japan).

Determination of *P. brasiliensis* cellular viability. The MTT metabolic assay was performed according to the method of Malavazi et al. (36), with some modifications. Cells were washed three times with PBS, and the amount equivalent to 400 micrograms of total protein was added to each well with 10 μl of MTT solution (5 mg/ml in PBS) in a final volume of 160 μl. The mixture was incubated in the dark for 2 h at 37°C, and after that, the 96-well plate was centrifuged at 3,600 × *g* for 10 min. The content of each well was removed, and 150 μl of isopropanol containing 5% (vol/vol) 1 M HCl was added to dissolve the formazan crystals. After 12 h of incubation in the dark at room temperature, the optical density was measured spectrophotometrically with a microtiter plate reader at 570 nm. All the MTT determinations were done in quadruplicate; the results are expressed as percentages of the values (mean) compared to the values observed at time zero for the control culture (100%). Aliquots from the control group were fixed with 4% paraformaldehyde (in PBS) or heat killed by autoclaving in order to obtain the values for nonviable cells.

Growth of the *P. brasiliensis* yeast form in the presence of mitochondrial respiratory chain inhibitors and inducers of oxidative stress. *P. brasiliensis* yeast cells were initially grown to the mid-exponential growth phase in a liquid PGY medium at 35.5°C. Cells were harvested by centrifugation, washed twice using fresh medium, resuspended in the same medium that contained the inhibitors or inducers to be tested, and then incubated for 12 h at 35.5°C. After this first incubation, the compounds were readded to the cultures and then incubated under the same conditions for 1 h. The cells were harvested by centrifugation, washed twice in sterile water, and processed for RNA isolation and real-time PCR assays. The concentrations of the compounds after single additions were as follows: 30 mM H_2O_2, 0.5 mM menadione, 1 mM SNP, 2 μM rotenone, 500 μM flavone, 1 mM KCN, 1.8 μM antimycin A, and 2 mM SHAM. In some flasks, compounds were added in combinations, such as KCN-SHAM, antimycin A-SHAM, rotenone-SHAM, rotenone-KCN, and menadione-SNP. DMSO and ethanol were also tested in order to determine their possible impact on gene expression levels.

Determination of carbonylated protein levels during the M-to-Y differentiation of *P. brasiliensis*. Oxidative modification of proteins by oxygen free radicals was monitored by Western blot analysis of carbonyl groups by use of an OxyBlot protein oxidation detection kit (Chemicon International, Inc.) as previously described (10, 68). Both treated and control cultures had the total proteins extracted by homogenization liquid nitrogen in a buffer containing 50 mM Tris-HCl, pH 7.4, 1 mM EGTA, 0.2% Triton X-100, 1 mM benzamidine, and 10 mg/ml each of leupeptin, pepstatin, and aprotinine. The homogenates were clarified by centrifugation at 20,800 × *g* for 60 min at 4°C. Total protein concentrations were determined by the Bradford method, and 20 μg was subjected to derivatization with dinitrophenylhydrazine (DNPH). About 10 μg of proteins was loaded into a 12% (wt/vol) SDS-PAGE gel and electroblotted to a nitrocellulose membrane. The membrane was incubated with the antibody anti-DNPH moiety of the proteins, and the immunoblot was detected by a chemiluminescent reaction. Densitometric analysis was performed by using the Image J program (available at http://rsbweb.nih.gov/ij/download.html).

Measurement of intracellular ROS in *P. brasiliensis* yeast form and *S. cerevisiae* cells. Intracellular ROS levels were determined as previously described by Ruy et al. (56) and Magnani et al. (34), with some modifications. Changes in the fluorescence of the probe 5-(and 6-) chloromethyl-2′,7′-dichlorodihydrofluorescein diacetate, acetyl ester (CM-H_2DCFDA) (Invitrogen) due to oxidation by

ROS were monitored using a Hitachi F-4500 fluorescence spectrophotometer at 30°C under agitation. The excitation and emission wavelengths were 503 and 529 nm, respectively. Assays were performed using 5×10^6 cells/ml of spheroplast cells from both *P. brasiliensis* and *S. cerevisiae* in 1.8 ml of a standard incubation medium that contained 0.6 mM sucrose, 10 mM HEPES-KOH at a pH of 7.2, 5 mM $MgCl_2$, 2 mM KCl, and 0.5 mM EGTA. The incubation medium was supplemented with the following oxidizable substrates: 10 mM pyruvate, 10 mM malate, 10 mM glutamate, 10 mM succinate, and 2 mM NADH. Other additions are described in the figure legends.

PCR cloning and recombinant plasmid construction. In order to clone and characterize *Pbaox* (GenBank accession number EEH19342), its sequence was initially amplified by PCR from both cDNA and genomic DNA templates by use of specific primers: 5′-CCCTAAGCTTACCATGGATCC-3′ (forward) and 5′-GGGTTCCTCGAGCATTTTA-3′ (reverse). The PCR products were then ligated into the plasmid PCR2.1-TOPO (Invitrogen). Several clones were sequenced so as to exclude any possible nucleotide mutation during PCR amplification. Inserts that were amplified from cDNA were transferred from PCR2.1-TOPO to pET28a(+) (Novagen) and pYES2-NCT (Invitrogen) expression vectors. pET28-*Pbaox* and the empty vector pET28a(+) were transformed into *E. coli* strain Rosetta(DE3)pLysS according to the method of Sambrook et al. (57a). pYES-*Pbaox* and the empty vector pYES2-NCT were transformed into *S. cerevisiae* by use of the lithium acetate method (61).

Analysis of nucleotide and amino acid sequences. *Pbaox* cDNA and genomic DNA sequences as well as the deduced amino acid sequences were analyzed to determine the presence of possible intron regions, *trans*-membrane domains, and mitochondrial signal peptides by use of previously described methods (67). The bioinformatics tools that were used in these analyses are available at http://workbench.sdsc.edu/ (tools using, e.g., the method of Kyte and Doolittle [30], isoelectric point determination, and the ClustalW algorithms) and at http://www.cbs.dtu.dk/services/SignalP/ (tools using, e.g., the SIGNALP 3.0 server [3]).

Heterologous expression of *Pbaox* in *S. cerevisiae* and *E. coli*. The expression of *Pbaox* in the *E. coli* strain Rosetta(DE3)pLysS was induced by the addition of 0.5 mM isopropyl-β-D-thiogalactopyranoside (IPTG) to the culture medium and incubation at 37°C for 12 h in an LB medium that had been supplemented with chloramphenicol (35 μg/ml) and kanamycin (35 μg/ml).

In *S. cerevisiae* cells, the expression of *Pbaox* was achieved by growing cells in a SC-URA$^-$ liquid medium that had been supplemented with 2% (wt/vol) galactose at 30°C for 24 h.

Immunodetection of *Pb*AOX. Protein samples from *E. coli* and *S. cerevisiae* mitochondria were obtained by sonication in 1% (wt/vol) sodium dodecyl sulfate (SDS). Proteins (50 μg) were mixed with a sample buffer that contained 125 mM Tris-HCl at a pH of 6.8, 20% (vol/vol) glycerol, 8% (wt/vol) SDS, 0.004% (wt/vol) bromophenol blue, and 100 mM DTT, which were then loaded and separated by SDS-PAGE (31), transferred to nitrocellulose membranes (Bio-Rad), and immunoblotted with a 1:300 dilution of mouse monoclonal antibodies that had been raised against the His_6 tag. The membranes were subsequently incubated with goat anti-mouse IgG that had been conjugated with horseradish peroxidase (HRP). Labeled proteins were visualized via incubation of the membranes with ECL Western blotting detection reagents (GE Healthcare).

Oxygen uptake measurements with *S. cerevisiae* and *E. coli*. Oxygen uptake was measured with a Clark-type electrode (72) that had been fitted to a Gilson oxygraph (Gilson Medical Electronics, Inc., Middleton, WI) in 1.8 ml of a standard incubation medium that contained 0.6 mM sucrose, 10 mM HEPES-KOH at a pH of 7.2, 5 mM $MgCl_2$, 2 mM KCl, and 0.5 mM EGTA at 30°C. The initial solubility of oxygen in the reaction buffer was considered to be 445 ng of atoms of O/ml (23). Further additions are indicated in the figure legends. DMSO and ethanol were also tested in order to determine any possible impact of these solvents on oxygen uptake. Respiratory parameters were determined as previously described (8).

RNA isolation, real-time PCRs, and reverse transcription-PCRs (RT-PCRs). Yeast cells were disrupted with glass beads and by grinding in liquid nitrogen (17) and immediately mixed with Trizol (Invitrogen) for RNA extraction in accordance with the supplier's recommendations. The absence of DNA contamination after RNase-free DNase treatment was verified by real-time PCR quantization of the *P. brasiliensis* α-tubulin gene *Ptub1* (http://143.107.203.68/pbver2/default.html) using oligonucleotides 5′-ACCCAGCTTGGAAACAGTGCT-3′ (forward) and 5′-CACGGACCATCAGCCTTCAAACC–6-carboxyfluorescein (FAM)–G-3′ (reverse).

All real-time PCRs were performed using an ABI Prism 7700 sequence detection system (Perkin-Elmer Applied Biosystems) as described by Semighini et al. (64). All *P. brasiliensis* real-time PCR products yielded a single band with the expected sizes according to visualizations on agarose gels (data not shown). Because there is no ideal control for gene expression, we first compared the α-tubulin and hexokinase gene probes as normalizers for the expressions of these genes. No difference was observed between the two normalizers. Accordingly, the α-tubulin gene was used to normalize all of the expression results (data not shown). Real-time PCR quantification of *ndh*2 (alternative NADH dehydrogenase gene; GenBank accession number CN240857), *nd*6 (complex I subunit 6 gene; GenBank accession number AY268589), and AOX (GenBank accession number EEH19342) was achieved using, respectively, the following LUX primers (Invitrogen): 5′-CTGGCGGAGAATGTTCCTGAT-3′ (forward) and 5′-CGGTGTCTCCCGTCCTGTACCAC–FAM–G-3′ (reverse), 5′-GCAGGAGGACCACTCGCTATG-3′ (forward) and 5′-CGGTTAGCTCTCCTGGCAGAAAC–FAM–G-3′ (reverse), and 5′-GCTGGTGTCCCTGGAATGGT-3′ (forward) and 5′-CGGGTCGATCCATCCATTATCC–FAM–G-3′ (reverse).

Statistical analysis. Statistical analysis for comparing the values that were obtained in the gene expression level experiments was performed with one-way analysis of variance (one-way ANOVA) followed by the Newman-Keuls *post hoc* test. The values that were obtained in the intracellular ROS generation experiments were compared using two-way ANOVA followed by Bonferroni's *post hoc* test. In both analyses, P values of <0.05 indicated significance. The software used for the calculations was GraphPad Prism, version 4.0, for Windows (GraphPad Software, Inc., San Diego, CA).

RESULTS

Effects of mitochondrial respiratory chain inhibitors on *P. brasiliensis* M-to-Y differentiation. After the characterization of oxidative phosphorylation in the yeast form of *P. brasiliensis* (40), we assessed the involvement of mitochondria in its M-to-Y differentiation using classical inhibitors of the mitochondrial respiratory chain and alternative pathways. Twenty-four hours after the temperature was shifted from 26°C to 35.5°C, chlamydospore-like structures were observed (48), which denote the start of the morphological changes from mycelia to yeast (Fig. 1) that were delayed by the presence of complex IV inhibitor KCN (the first chlamydospore-like structure observed after 48 h) (Fig. 1). In order to rule out the possibility that the compound was degraded during the course of the experiment, KCN was also added to the culture after 24 and 72 h, and no change was observed in relation to the inhibition pattern that corresponded with a single KCN addition (data not shown). Inhibitors of complex III (antimycin A) and AOXs (SHAM) delayed M-to-Y differentiation for up to 120 h (Fig. 1). Similarly to the assays with KCN, multiple additions of antimycin A or SHAM did not increase the inhibition of M-to-Y differentiation; however, the inhibition of complex III or IV with the simultaneous inhibition of AOX (Ant A-SHAM or KCN-SHAM) completely quenched M-to-Y differentiation (Fig. 1). The M-to-Y transition was quantified by counting the different morphotypes that are observed during this process. Morphological units were arbitrarily classified as hyphae, differentiating hyphae (characterized by the development of chlamydospore-like structures), transforming yeast (characterized by the production of multiple buds by the chlamydospore), and yeast. One day later, 75% of control cells had started the M-to-Y transition (Fig. 2A), but it took 3 days to obtain 75% of completely differentiated yeast cells (Fig. 2B). As shown in Fig. 1, the initiation of M-to-Y transition was delayed for up to 2 days by KCN and for up to 4 days by antimycin A or SHAM (Fig. 2). Ten days later, 75% of antimycin A-treated cells had completed the M-to-Y transition, but only 25% of the SHAM-treated cells had completed this process (Fig. 2B). On the other hand, the associations KCN-SHAM or antimycin A-SHAM completely blocked the M-to-Y transition (Fig. 2).

After 240 h and under the condition of simultaneous inhi-

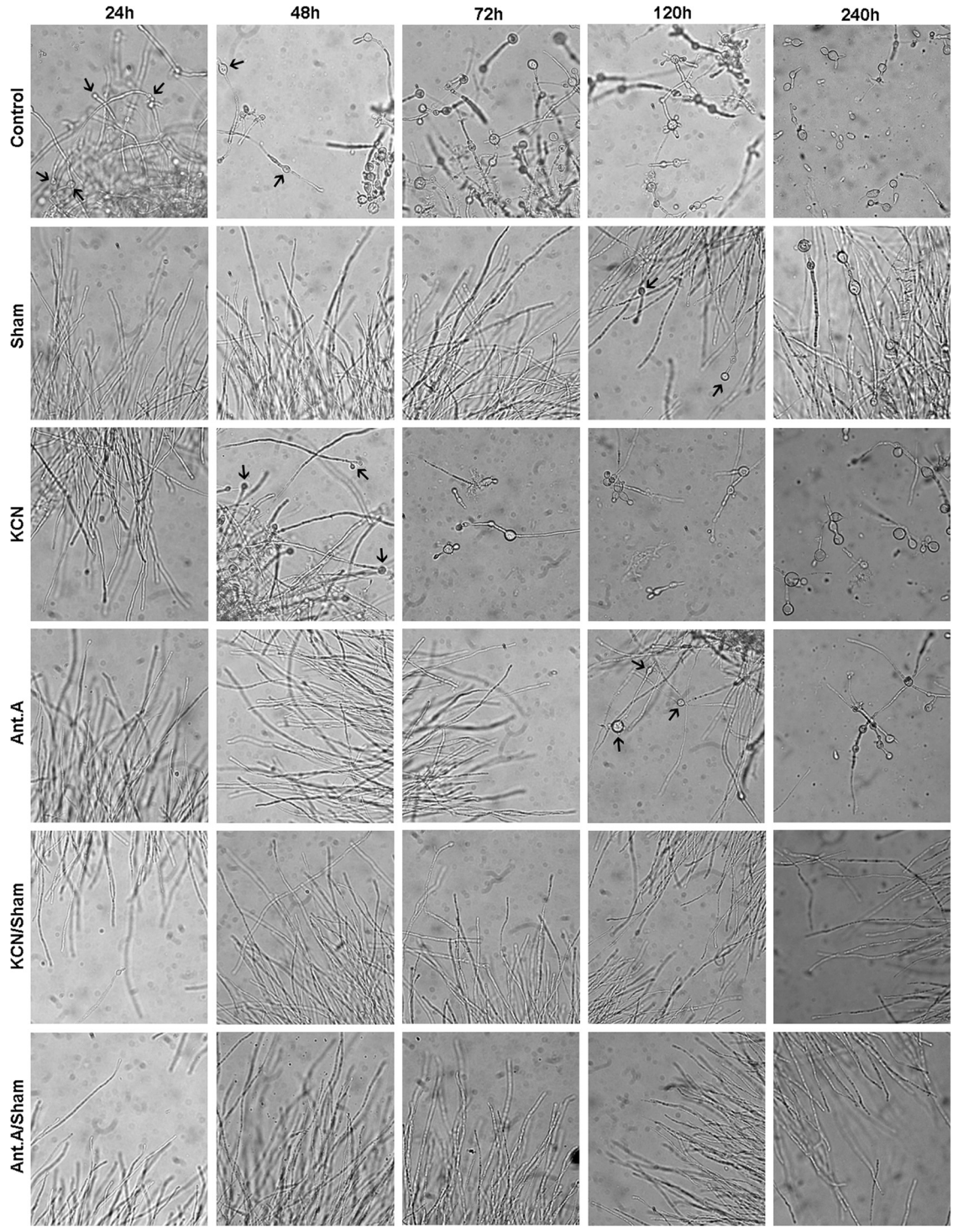

FIG. 1. Images of *P. brasiliensis* during M-to-Y differentiation in the presence of mitochondrial respiratory chain inhibitors. M-to-Y differentiation was induced as described in Materials and Methods. Mitochondrial respiratory chain inhibitors were added just before the temperature was shifted from 26°C to 35.5°C. Their concentrations per addition, even when combined, were as follows: for SHAM, 2 mM; for KCN, 1 mM; and for antimycin A, 1.8 μM. In some of the experiments, drugs were added once more after 24 or 72 h, but there were no noticeable differences between the results obtained with single additions and those obtained with multiple additions (data not shown). Images were selected from a single experiment that was representative of at least three independent experiments. Images were captured using a 40× objective lens, resulting in a final magnification of ×400, with an Olympus BX51 model U-LH100-3 microscope that was coupled to an Olympus model C-5060 wide-zoom digital camera. Black arrows indicate chlamydospores, which are characteristic structures during M-to-Y differentiation.

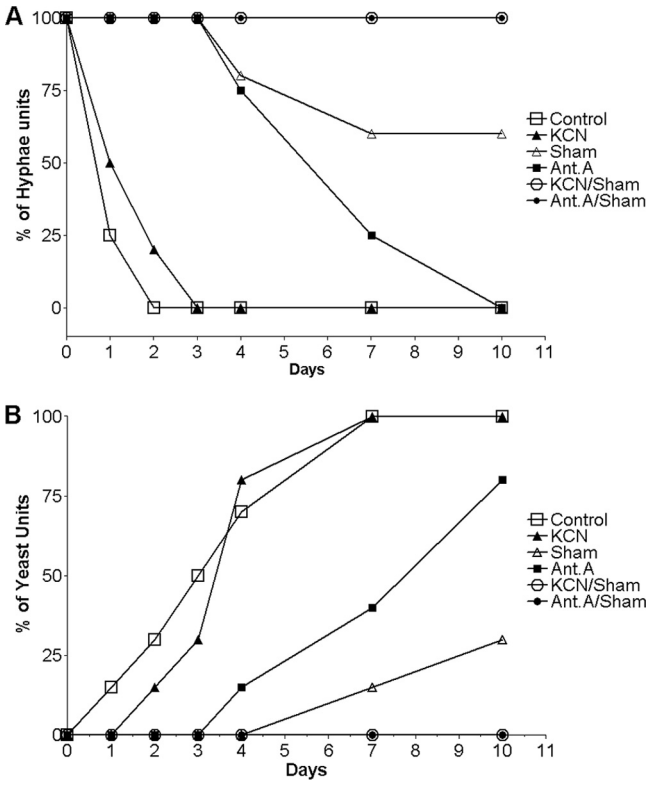

FIG. 2. Quantification of the M-to-Y differentiation. Morphological transformation was induced as described in Materials and Methods. At the different time points, morphological units were arbitrarily classified as hyphae, differentiating hyphae, transforming yeast, and yeast. Relative amounts of hyphae (A) and yeast (B) were obtained after individual scoring of at least 300 morphological units for each time point.

bition, mycelia that did not differentiate to yeast were harvested, washed twice with a fresh PGY medium, and incubated without inhibitors for an additional 240 h, and no culture was able to differentiate to yeast. Other respiratory chain inhibitors, such as rotenone (complex I) and flavone (alternative NADH dehydrogenases), or solvents, such as DMSO and ethanol, did not affect *P. brasiliensis* differentiation (data not shown). Moreover, none of the inhibitors that were used in the differentiation assays affected the vegetative growth of the *P. brasiliensis* yeast form (not shown). To verify whether the undifferentiated mycelia have been killed or just blocked by the inhibitors, we determined the viability of the cells during M-to-Y differentiation using the MTT assay. The viability of untreated cells was unaffected for the first 2 days of culture and then decreased until day 10, when the viability was 75% compared to the level observed at time zero (Fig. 3). Cells treated with SHAM had decreased viability on days 1, 3, and 4, when 60% of the cells were still viable, remaining stable after 10 days of culture (Fig. 3). KCN-SHAM- and antimycin A-SHAM-treated cells showed pronounceable decreases in viability compared to the levels for control and SHAM-treated cells throughout the 10 days of culture (Fig. 3). However, 7 days after 40% of the cells were still viable, which was lower than the level of viability for the control cells but considerably higher than the level of viability for heat-killed or fixed cells

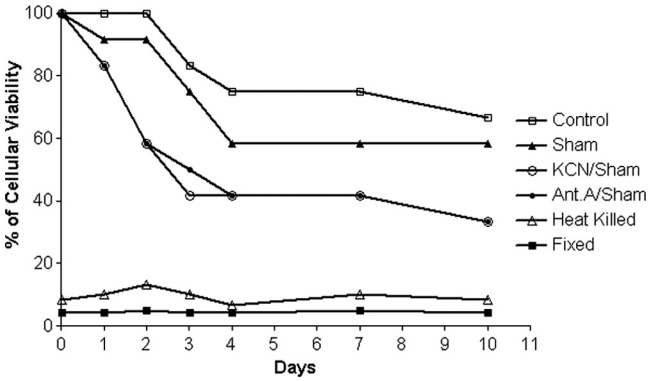

FIG. 3. Cellular viability during M-to-Y differentiation. Cells under different treatments were harvested and processed as described in Materials and Methods. All the MTT determinations were done in quadruplicates. The values plotted on the graphs were obtained using the means of results from the quadruplicates; these values represent the percentages observed at the different time points compared to the value observed for the control cells at time zero.

(values comparable to those observed for the background with the MTT method) (Fig. 3).

Expression of *Pbaox* during M-to-Y differentiation and the vegetative growth of the yeast form. Because inhibitors of mitochondrial AOX interfered with the *P. brasiliensis* differentiation process, we assessed the expression levels of *Pbaox* during M-to-Y differentiation and the vegetative growth of the yeast form. The *Pbaox* transcript levels increased by 345% after 10 h of incubation at 35.5°C in cells that were differentiating in a complete medium and decreased to their lowest levels (25% of the expression levels observed at time zero) at 48 h (Fig. 4A). A second increase in *Pbaox* transcript levels was observed after 72 h, and higher levels, which were comparable to those achieved at 10 h, were reached after 240 h. In cells that were differentiating in a minimal medium, the first peak of *Pbaox* expression was delayed (48 h) in comparison to the level for cells that were grown in a complete medium (Fig. 4A). Additionally, in a minimal medium, the second peak of expression was not observed for up to 240 h (Fig. 4A).

We observed that the expression levels of *Pbaox* were modulated during the growth curve of the *P. brasiliensis* yeast form. The expression of *Pbaox* was lower in the first 24 h as well as during the stationary growth phase (120 and 240 h) (Fig. 4B). On the other hand, the *Pbaox* transcript levels exhibited a gradual increase from 48 to 96 h to levels that were nearly 3-fold higher than those at zero time and 24 h and those in the stationary phase (Fig. 4B). This period of higher levels of *Pbaox* expression corresponds to the early- and mid-exponential phases of growth for the yeast form.

Oxidative stress during M-to-Y differentiation of *P. brasiliensis*. It has been proposed that oxidative stress conditions upregulate the expression of AOX genes. In order to evaluate this hypothesis, we measured oxidative stress during M-to-Y differentiation by determining the levels of protein carbonylation. Proteins were isolated from control and SHAM-treated cells throughout 10 days of culture and then processed. There was an increase of carbonylated proteins during M-to-Y differentiation as shown by the intensity of the bands at days 1, 2, and 3 (around 50% increased), day 4 (150%), and day 10

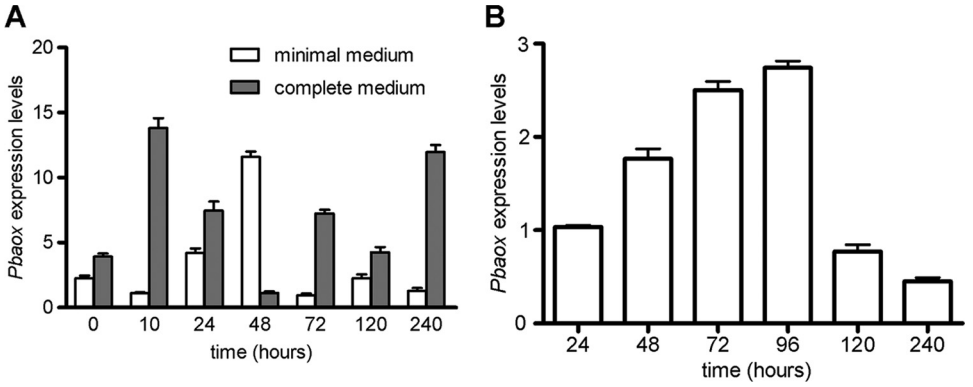

FIG. 4. Expression levels of *Pbaox* during M-to-Y differentiation and growth curve of the yeast form. The number of transcripts was determined by real-time PCR as described in Materials and Methods and normalized by the number of α-tubulin transcripts. (A) Cells growing in the minimal medium (white bars) or complete medium (gray bars). M-to-Y differentiation was induced as described in Materials and Methods. (B) Yeast cells were grown in a complete medium at 35.5°C. The values for the *Pbaox* expression levels are the averages ± standard errors of the means (SEMs) of results from three independent assays. The statistical analyses are described in Materials and Methods.

(50%), in comparison to the level observed for the band at time zero (Fig. 5, left panels). The increase of carbonylated proteins was even higher when the M-to-Y differentiation occurred under the inhibition of AOX by SHAM (Fig. 5, right panels). All time points analyzed under this condition showed increased levels of carbonylated proteins, with the values ranging from 1.5 to 3.5 times higher than those observed at time zero (Fig. 5B; see also Fig. S1B in the supplemental material).

Effects of oxidative stress on the expression of mitochondrial respiratory chain genes in the yeast form. We challenged *P. brasiliensis* yeast cells with different compounds that are known to generate ROS and RNS and measured the corresponding *Pbaox* expression levels. In comparison to untreated control cells, SNP- and KCN-treated cells exhibited nonsignificant increases in *Pbaox* expression (Fig. 6A). H_2O_2, rotenone, rotenone-KCN, and antimycin A treatments caused 2-fold increases in *Pbaox* expression, whereas menadione and menadione-SNP increased the levels of *Pbaox* transcripts by almost 3- and 4-fold, respectively (Fig. 6A); however, SHAM, which is a specific inhibitor of AOXs, did not significantly impact the expression of *Pbaox* (Fig. 6A). DMSO and ethanol did not impact *Pbaox* transcript levels (data not shown).

Next, we investigated the effect of these inhibitors on subunit 6 of complex I (*Pbnd*-6) because it is an important generator of ROS in mitochondria. Most of the compounds had no significant impact on *Pbnd*-6 gene expression, except for menadione-SNP, which increased *Pbnd*-6 expression levels 6-fold (see Fig. S1 in the supplemental material).

Effects of mitochondrial respiratory chain inhibitors on the generation of intracellular ROS in yeast cells of *P. brasiliensis*. Some mitochondrial respiratory chain inhibitors could potentially upregulate the expression of *Pbaox.* In order to verify whether these compounds also increased the intracellular status of oxidative stress in *P. brasiliensis* yeast cells, we measured intracellular ROS generation by using the CM-H_2DCFDA fluorescent probe. Ten minutes after the addition of the inhibitors to the reaction medium, a slight increase in the intracellular ROS content was observed in comparison to the level for the control cells (Fig. 6B); however, after 40 min, the cells that had been treated with antimycin A and rotenone exhibited higher levels of intracellular ROS (80% and 65%, respectively) (Fig. 6B). KCN did not increase intracellular ROS generation (Fig. 6B), which is consistent with its inability to increase the expression of *Pbaox* (demonstrated in Fig. 6A). It was not possible to test AOX inhibitors, because they interfere with this ROS assay (56).

Cloning, sequence analysis, and heterologous expression of *Pbaox*. We cloned and heterologously expressed *Pbaox* in order to investigate its function during the differentiation process and pathogenesis of the fungus.

Analyses of *Pbaox* demonstrated a coding sequence of 1,136 bp, which carries an open reading frame of 1,059 bp that encodes 352 amino acids with a predicted molecular mass of 40.3 kDa and a theoretical isoelectric point of 9.25. The alignment of cDNA and genomic DNA sequences revealed the presence of a 77-bp intron region from nucleotides 262 to 339 (see Fig. S2 in the supplemental material). Alignments of the deduced *Pb*AOX amino acid sequence with AOXs from *H. capsulatum*, *Neurospora crassa*, *Candida albicans*, and *Trypanosoma brucei brucei* showed 72%, 46%, 40%, and 29% similarities, respectively (Fig. S3), including two hydrophobic regions (W147 to R169 and W209 to L231) (Fig. S2) and the four primary conserved regions among the AOXs (LET, NERMHL, LEEA, and RADE-H) (Fig. S3) that contain the metal-binding amino acids E155, E194, H197, E245, E300, and H303 and the ubiquinone-binding amino acids Y230 and Y252 (44, 66).

Pbaox was subcloned into the expression vector pET28a(+) for expression in *E. coli* cells and into pYES2-NTC for expression in *S. cerevisiae*. The final constructs were named pET28-*Pbaox* and pYES-*Pbaox*. The expected protein sizes were 42 kDa in *E. coli* (*Pb*AOX plus an N-terminal His tag) and 48 kDa (*Pb*AOX plus an N-terminal and C-terminal His tags) in *S. cerevisiae*. The expression of *Pb*AOX was confirmed by Western blotting via an anti-His tag antibody (Fig. 7D and 8D). In isolated *S. cerevisiae* mitochondria, a band was detected at the expected size (48 kDa) in addition to a smaller band at around 42 kDa that corresponded to the expected size without the mitochondrial signal peptide (Fig. 7D, lane 3). In *E. coli*/pET28-*Pbaox* samples, a single band at the expected size (42 kDa) was detected (Fig. 8D, lane 3).

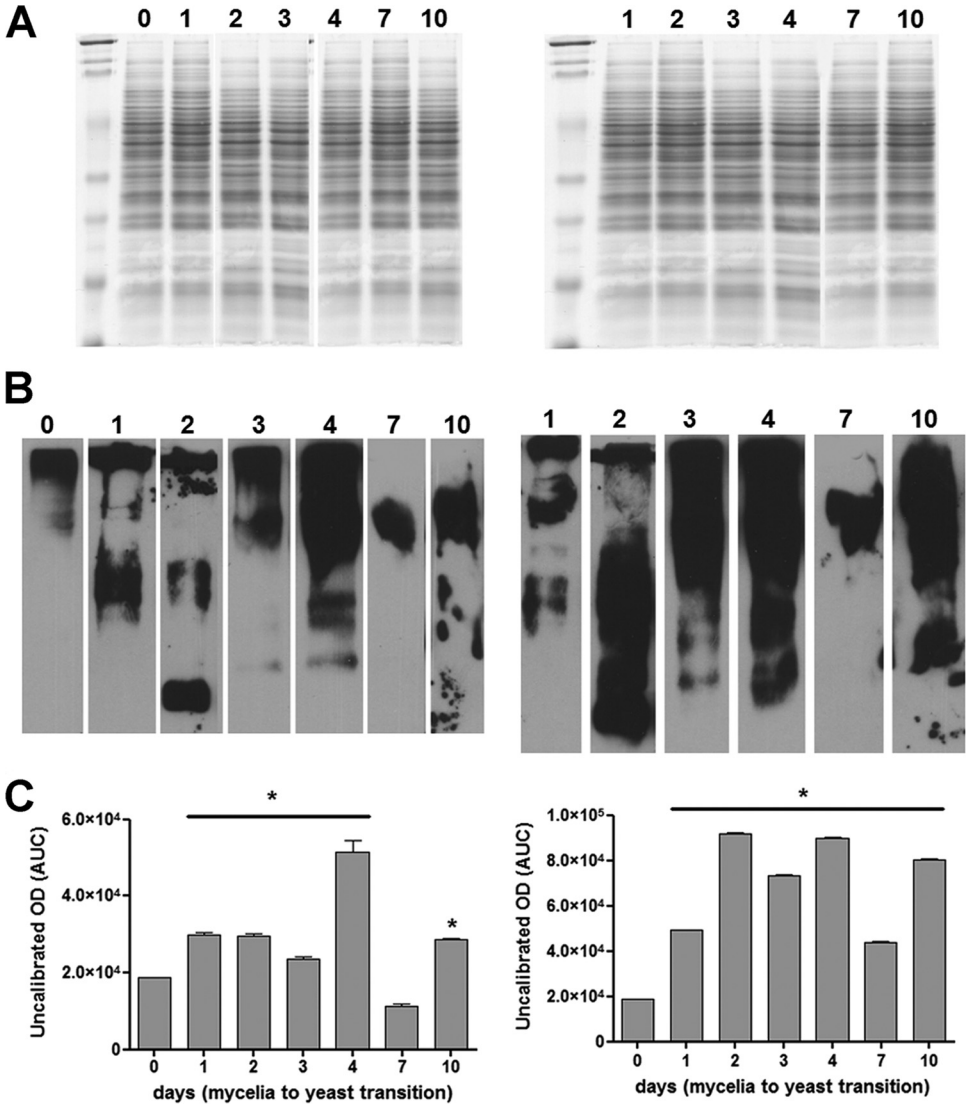

FIG. 5. Pattern of oxidative damaged proteins during M-to-Y differentiation. (A) Coomassie staining of SDS-PAGE gels. (B) Western blot probed with antibodies that recognize the DNPH moieties of carbonylated proteins. (C) Western blot densitometry of carbonylated proteins. The left and right panels show untreated cells and cells treated with SHAM, respectively. Asterisks indicate P values of <0.05, compared to the values observed at time zero. The numbers on top represent the days after the temperature shift and the beginning of M-to-Y conversion. Western blot images were analyzed as described in Materials and Methods, and the values for optical density, which represent the levels of oxidative damaged proteins, were plotted in the graphs. AUC, area under the curve.

Heterologous expression of *Pbaox* confers cyanide-resistant respiration to *S. cerevisiae* and *E. coli* cells. The polarographic measurement of oxygen uptake by *E. coli* and *S. cerevisiae* in both *Pb*AOX-expressing and control cells showed that KCN completely inhibited oxygen uptake in *S. cerevisiae*/pYES (Fig. 7C) and *E. coli*/pET28 (Fig. 8C) cells that did not overexpress *Pb*AOX; however, KCN only partially inhibited oxygen uptake in *Pb*AOX-overexpressing *S. cerevisiae*/pYES2-*Pbaox* (Fig. 7A) and *E. coli*/pET28-*Pbaox* (Fig. 8A) cells. Moreover, the addition of SHAM or BHAM (specific inhibitors of AOXs) partially inhibited oxygen uptake in *S. cerevisiae*/pYES2-*Pbaox* (Fig. 7B) and *E. coli*/pET28-*Pbaox* (Fig. 8B) cells. These agents also inhibited KCN-resistant respiration and quenched oxygen uptake in *Pb*AOX-overexpressing *S. cerevisiae*/pYES2-*Pbaox* (Fig. 7A) and *E. coli*/pET28-*Pbaox* (Fig. 8A) cells.

***S. cerevisiae Pbaox*-expressing cells exhibited compromised cell growth and a decreased intracellular ROS generation.** *Pbaox* overexpression and activity were confirmed for both *S. cerevisiae* and *E. coli* cells. In order to determine the influence of *Pb*AOX activity in *S. cerevisiae* cells, we evaluated their growth curves and intracellular ROS generation. *Pb*AOX-overexpressing cells exhibited a lower growth rate and lower cell numbers during both exponential and stationary stages in both fermentable (see Fig. S5A in the supplemental material) and nonfermentable (Fig. S4B) media.

The intracellular oxidative status of *S. cerevisiae* cells was determined via a CM-H_2DCFDA fluorescent probe. As can be observed in Fig. 9, the fluorescence measured in *S. cerevisiae*/pYES cells after 10, 30, and 50 min increased by approximately 25%, 50%, and 75%, respectively. An increase in fluorescence

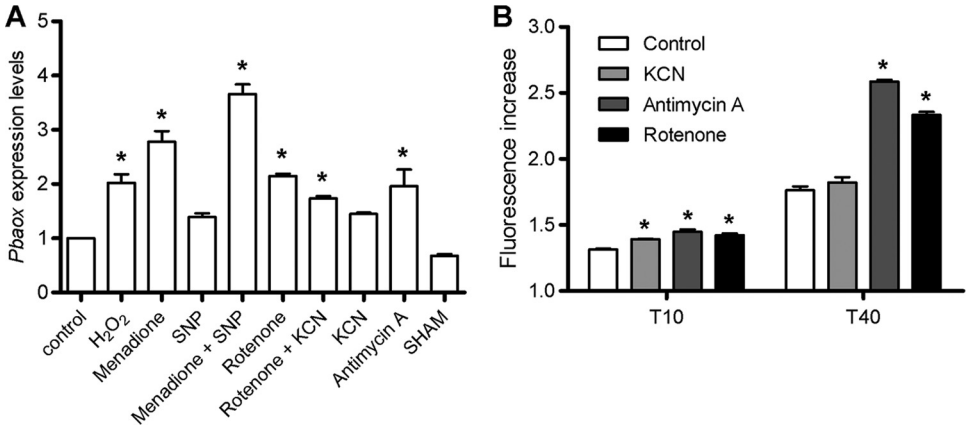

FIG. 6. The effect of ROS/RNS-generating compounds on the expression levels of *Pbaox* and the generation of intracellular ROS during the exponential growth phase of *P. brasiliensis* yeast cells. (A) Cell cultures and ROS/RNS-generating compound challenges were performed as described in Materials and Methods. The number of *Pbaox* transcripts was determined and normalized as previously described. The concentrations of the compounds in each addition were as follows: for H_2O_2, 30 mM; for menadione, 0.5 mM; for SNP, 1 mM; for rotenone, 2 μM; for KCN, 1 mM; for antimycin A, 1.8 μM; and for SHAM, 2 mM. These values represent the expression levels relative to the level for the control and are presented as averages ± SEMs of results from three independent assays. (B) Cell culture, spheroplast generation, and ROS measurement procedures were performed as described in Materials and Methods. Spheroplast cells (5×10^6 cells/ml) were loaded with the CM-H_2DCFDA fluorescent probe (5 μM) for 30 min at 37°C. The oxidation of the probe by ROS was monitored using a Hitachi F-4500 fluorescence spectrophotometer at 30°C under agitation. The excitation and emission wavelengths were 503 and 529 nm, respectively. The concentrations of the inhibitors in each addition were as follows: for KCN, 1 mM; for antimycin A, 1.8 μM; and for rotenone, 2 μM. The values for fluorescence represent increases at 10 and 40 min in comparison to the value observed at time zero (before the addition of inhibitors), and these values are shown as the averages ± SEMs of results from three independent assays. Asterisks indicate *P* values of <0.05. The statistical analyses are described in Materials and Methods.

in *S. cerevisiae*/pYES-*Pbaox* cells was also observed, although this increase was significantly lower than those that were observed in cells that were not expressing *Pb*AOX at 30 and 50 min. Similarly to the data that were obtained from *P. brasiliensis* yeast cells (Fig. 6B), the exposure of *S. cerevisiae* to KCN did not increase ROS generation in comparison to that in control cells, even though the level of ROS after 50 min was significantly lower in *Pb*AOX expressing-cells that were exposed to KCN than in control cells. Antimycin A increased ROS generation by 50%, 75%, and 150% after 10, 30, and 50

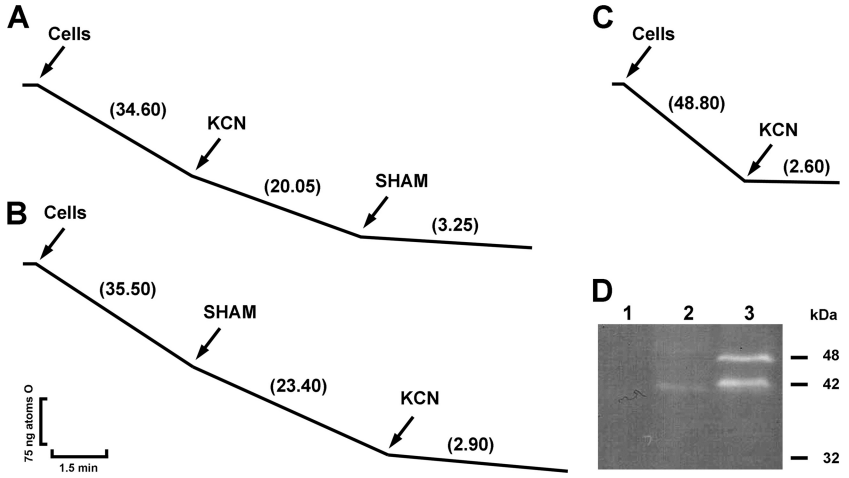

FIG. 7. KCN-resistant respiration in *S. cerevisiae* expressing the *Pbaox* gene. (A and B) *S. cerevisiae*/pYES-*Pbaox*-induced cells. (C) *S. cerevisiae*/pYES. Five million cells/ml were incubated at 30°C in 1.8 ml of a respiration medium. At the indicated time points, KCN (1 mM) and SHAM (2 mM) were added. The rate of oxygen uptake was expressed as ng atoms of oxygen/min. All the assays were performed with 5×10^6 cells/ml. The depicted graphs are representative of at least three independent assays. (D) Reverse image of the immunodetection of *Pb*AOX in *Pbaox*-expressing *S. cerevisiae*. Fifty micrograms of mitochondrial protein was loaded per lane. Mitochondria were isolated during the exponential growth phase, as described in Materials and Methods, from *S. cerevisiae* cells that had been transformed with empty vector (lane 1), *S. cerevisiae*/*Pbaox*-uninduced cells (lane 2), and *S. cerevisiae*/*Pbaox*-induced cells (lane 3). SDS-PAGE and Western blot techniques were performed as described in Materials and Methods. His-tagged *Pb*AOX was detected using a monoclonal antibody that was raised against the His tag. The expected molecular mass for the final protein with the signal peptide and His tag is approximately 48 kDa, whereas that for the final protein without the signal peptide is approximately 42 kDa.

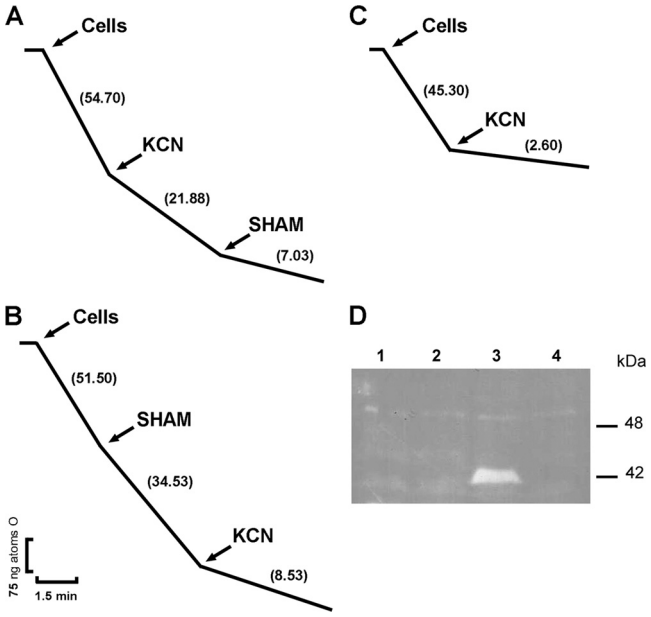

FIG. 8. Cyanide-resistant respiration in *Pbaox*-expressing *E. coli*. (A and B) *E. coli*/pET28-*Pbaox*-induced cells. (B) *E. coli*/pET28. Cells were incubated at 30°C in 1.8 ml of a respiration medium. At the indicated time points, KCN (1 mM) and SHAM (2 mM) were added. The rate of oxygen uptake was expressed as ng atoms of oxygen/min. All the assays were performed with 0.2 mg/ml of proteins. The depicted graphs are representative of at least three independent assays. (D) Reverse image of the immunodetection of *Pb*AOX in *Pbaox*-expressing *E. coli*. Fifty micrograms of protein was loaded per lane. Samples were prepared, as described in Materials and Methods, from induced *E. coli* cells that had been transformed with the empty vector (lane 1), uninduced *E. coli* cells that had been transformed with the empty vector (lane 2), induced *E. coli* cells that had been transformed with pET28-*Pbaox* (lane 3), and uninduced *E. coli* cells that had been transformed with pET28-*Pbaox* (lane 4). SDS-PAGE and Western blot techniques were performed as described in Materials and Methods. His-tagged *Pb*AOX was detected using a monoclonal antibody that was raised against the His tag. The expected molecular mass for the final protein is about 42 kDa.

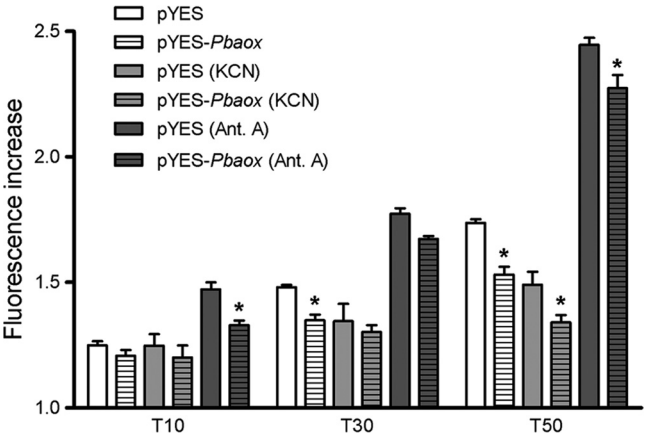

FIG. 9. The heterologous expression of the *Pbaox* gene decreases the generation of intracellular ROS in *S. cerevisiae* cells. Cell culture, induction of *Pbaox* expression, spheroplast generation, and ROS measurement procedures were performed as described in Materials and Methods. The spheroplasts of *S. cerevisiae*/pYES-*Pbaox* and *S. cerevisiae*/pYES cells (5×10^6 cells/ml) were loaded with the CM-H_2DCFDA (5 μM) fluorescent probe for 30 min at 37°C. The oxidation of the probe by ROS was monitored using a Hitachi F-4500 fluorescence spectrophotometer at 30°C under agitation. The excitation and emission wavelengths were 503 and 529 nm, respectively. The concentrations of the inhibitors in each addition were as follows: for KCN, 1 mM, and for antimycin A, 1.8 μM. The values represent increases in fluorescence at 10, 30, and 50 min in comparison to that at time zero (before the addition of inhibitors), and these values are shown as the averages ± SEMs of results from three independent assays. Asterisks indicate P values of <0.05 between *S. cerevisiae*/pYES-*Pbaox* and *S. cerevisiae*/pYES cells. The statistical analyses are described in Materials and Methods.

min, respectively. Nevertheless, *Pb*AOX-expressing cells that were exposed to antimycin A exhibited a lower level of fluorescence than control cells (Fig. 9).

DISCUSSION

Infection by *P. brasiliensis* and the establishment of PCM are closely associated with M-to-Y differentiation during the interaction of the fungus with its mammalian hosts. After being phagocytosed by macrophages, microbes are exposed to ROS and RNS as well as to the action of lysosomal enzymes following phagolysosomal fusion. Despite the efforts of the host immune system, dimorphic fungal pathogens can occasionally establish and cause infection. If untreated, this infection can develop into systemic mycoses, which are particularly a problem for immunocompromised and immunosuppressed individuals (51). On the pathogen side, the regulated spatial and temporal generation of ROS is related to fungal cellular differentiation and development, which is thought to rely on MAP kinase (MAPK) signal transduction pathways (63). Recently, it has been proposed that the MAPK cascade could be involved in the sensing of different stresses in dimorphic fungi, including temperature, osmotic or oxidative stress, nutrient deprivation, redox potential, and host-derived factors (46). Therefore, it is important to assess the possible correlations that exist between mitochondrial function, ROS generation, and fungal development processes in *P. brasiliensis*.

Mitochondria are the primary intracellular sources of ROS, which have the potential to damage biomolecules and interfere with cellular processes (20–22). In order to protect from these deleterious effects of ROS, fungal cells have developed a series of mechanisms to reduce ROS levels (15). In some plants and fungi, the mitochondrial respiratory chain possesses alternative pathways in addition to proton-pumping complexes in order to prevent ROS generation, specifically, alternative NADH-ubiquinone oxidoreductases and alternative ubiquinol oxidases (AOXs) (28). Alternative NADH-ubiquinone oxidoreductases are located in the mitochondrial matrix, wherein they oxidize internal NADH, or are alternatively located in the intermembrane space, wherein they could oxidize cytosolic NADH and/or NADPH (29). Alternative ubiquinol oxidases directly transfer electrons from ubiquinol to oxygen. AOXs have been documented to occur in plants (4, 65, 74), algae (71), yeasts (75), free-living amoebae (25), and protozoa (69) as well as in pathogenic fungi, such as *Aspergillus fumigatus* (72), *H. capsulatum* (27, 38), and *P. brasiliensis* (17, 39, 40, 42).

The inhibition of complex III and/or AOX, which interferes with ROS homeostasis, was observed to affect the M-to-Y differentiation of *P. brasiliensis*. The inhibition of AOX has

been reported to affect the development and/or differentiation of several pathogens, such as *C. albicans* (56), *Cryptosporidium parvum*, *T. gondii*, *Plasmodium falciparum* (55), and *T. brucei brucei* (47); however, it is still unclear whether the killing of these microorganisms due to mitochondrial respiratory chain inhibition occurs by energy deficiency, ROS generation/cell damage, or both.

It has been reported that in *P. brasiliensis*, several genes that relate to bioenergetic processes (mitochondrial and cytosolic) are modulated in a pattern that suggests a more favorable aerobic metabolism in the mycelial phase and fermentative metabolism in the yeast phase (11, 12, 48). Conversely, the upregulation of genes related to mitochondrial functions during the yeast phase of *P. brasiliensis*, such as the cytochrome *c* oxidase complex (1), ATP synthase (7), NADH-ubiquinone oxidoreductase (complex I), and alternative NADH-ubiquinone oxidoreductase (40), as well as the electron transfer flavoprotein-ubiquinone oxidoreductase, which is a component of complex III (14), has been reported.

In a previous work, we characterized, *in situ*, the oxidative phosphorylation processes of *P. brasiliensis* mitochondria during the yeast phase (40). We demonstrated the presence and activity of a complete mitochondrial respiratory chain (complexes I to V) as well as an alternative NADH-ubiquinone oxidoreductase and an AOX. Our previous and present results in combination with previous literature (1) suggest that *P. brasiliensis* can perform aerobic and anaerobic respiration in both morphological forms. In this regard, it has been reported that, upon phagocytosis, there is a shift from fermentative to nonfermentative metabolism in intracellular pathogens, which may use two-carbon compounds from fatty acid degradation for energy production via the glyoxylate cycle (2, 13, 19, 32, 33, 62). Indeed, the upregulation of genes from the glyoxylate cycle has been reported to occur during the M-to-Y differentiation of *P. brasiliensis* in culture medium (11, 12, 17, 48) and upon the internalization of *P. brasiliensis* by murine macrophages (9, 70). Additionally, nutritional stress conditions have been observed to influence the expression levels of the glyoxylate cycle-related genes of cultured yeast cells (9). In this regard, the upregulation of *Pbaox* during the first hours of M-to-Y differentiation and during the exponential growth of the yeast form could be associated with fatty acid degradation. This might occur by a decreased overflow of electrons in the mitochondrial respiratory chain and/or in association with the external alternative NADH-ubiquinone oxidoreductase involving the oxidation of cytosolic NADH that is generated in the glyoxylate cycle or in fermentative pathways, which subsequently balance the cytosolic redox potential, as we previously suggested (40). It had been reported that *H. capsulatum*, *Blastomyces dermatitidis*, and *P. brasiliensis* possess three different respiratory phases during morphogenesis (37, 42). After the temperature shift, there is an uncoupling of oxidative phosphorylation and a progressive decrease of respiration (stage 1). The dormant period (stage 2) occurs from between 24 and 40 h to 6 days, which is characterized by decrease in the concentrations of mitochondrial electron transport components. Finally, stage 3 is characterized by restoration of cytochrome components, normal respiration, induction of a cytosolic cysteine oxidase, and completion of the transition to yeast morphology (43, 57). During stage 2, cysteine and other sulfhydryl compounds are able to induce the shunt pathways utilizing cytochrome oxidase and alternative oxidase, which is inhibited by cyanide and SHAM but is resistant to antimycin A inhibition (57). It is speculated that the inactivation of mitochondrial respiration during stage 2 results from a temperature-induced increase in oxidation-reduction potential; under this condition, the sulfhydryl compounds would act as reducing agents, which may be required for maintenance of the activity of the remaining mitochondrial components (37). In accordance with these previous reports, our findings show that there is an increase in the carbonylated proteins (oxidative stress) during M-to-Y transition, which is correlated with the upregulation of *Pbaox*. It has been reported that AOXs are upregulated in fungi that are under mitochondrial respiratory chain inhibition and/or oxidative stress conditions (24, 27, 28, 35). In agreement, our data show that *Pbaox* expression is also upregulated by ROS/RNS-generating compounds and mitochondrial respiratory chain inhibitors. The higher level of induction of *Pbaox* expression after the inhibition of complex I by rotenone and complex III by antimycin A may relate to the increased ROS generation upon inhibition of these complexes. Indeed, rotenone and antimycin A were observed to cause intracellular oxidative stress in the yeast cells of *P. brasiliensis*. Apparently, the regulation of *Pbaox* expression relates more to intracellular oxidative status than to electron flow (solely) in the respiratory chain. The AOX-specific inhibitor SHAM did not affect *Pbaox* expression, suggesting that *Pb*AOX activity does not control its own expression. Nevertheless, the inhibition of complex I by rotenone increased the expression of its own subunit 6, which is similar to what has been observed for other oxidative-stress-generating compounds (see Fig. S2 in the supplemental material).

We demonstrated that SHAM and antimycin A delayed the M-to-Y transition and that SHAM-antimycin A and SHAM-KCN associations promoted a complete and irreversible inhibition of the M-to-Y conversion. These effects may be associated with the increase of oxidative stress inside the cells, as suggested by the higher levels of carbonylated proteins in SHAM-treated cells during M-to-Y conversion. It was previously demonstrated that *p*-chloromercuriphenylsulfonic acid (PCMS), a sulfhydryl inhibitor, permanently and irreversibly blocked the M-to-Y transition in *H. capsulatum* (43). Thus, it is reasonable to assume that extreme alterations of the intracellular redox balance at early stages of the M-to-Y transition may affect crucial steps for the differentiation of dimorphic fungi.

Pbaox and its expression (17) and AOX activity (40, 42) have previously been described for *P. brasiliensis*; however, the characterization of the *Pbaox* gene and protein sequences, as well as its heterologous activity in eukaryotic and prokaryotic systems, is described here for the first time. As demonstrated, *Pbaox* is very similar to other fungal AOXs in terms of its nucleotide and amino acid sequences, catalytic domains, and *trans*-membrane regions.

The heterologous expression of *Pbaox* in *S. cerevisiae* demonstrates that the protein was correctly processed and targeted to the mitochondria, as demonstrated by Western blot analysis. The presence of a second band with a molecular size that corresponds to a combination of *Pb*AOX before peptide signal cleavage and two histidine tags (N and C terminals) is understandable, because most mitochondrial preparations are en-

riched fractions; therefore, the presence of vesicles and other cytosolic structures is not insignificant. Moreover, the presence of KCN-resistant respiration in *Pbaox*-expressing cells confirms that the heterologous protein was functional. In bacteria, we were also able to express *Pb*AOX as a functional enzyme, as demonstrated by Western blotting (Fig. 8) and the presence of KCN-resistant respiration in *Pbaox*-expressing bacteria (Fig. 8). Interestingly, this KCN-resistant respiration arrested growth in *S. cerevisiae* cells under culturing in both fermentable and nonfermentable media (see Fig. S5 in the supplemental material). A similar effect was previously described for *S. cerevisiae* via the overexpression of a heterologous AOX from the yeast *Hansenula anomala* (41). In that study, the increased levels of Krebs cycle enzymes in response to AOX energy-dissipating activity confirmed the close link between AOX and the cycle. The authors proposed that AOX has a direct effect in reducing substrate availability and a regulatory role in energy balance.

The present study demonstrates, for the first time, that heterologously expressed AOX in *S. cerevisiae* decreases intracellular ROS generation compared to the level for cells that bear only the empty vector. This finding supports the hypothesis that AOXs play an important role in intracellular redox balancing. *Pb*AOX is a unique enzyme in *P. brasiliensis* that is not present in its mammalian hosts. In this context, we have demonstrated that *Pb*AOX and other components of the mitochondrial respiratory chain are critical during the early stages of M-to-Y differentiation, which is an essential step for the pathogenesis and establishment of PCM. Therefore, *Pb*AOX is a potential chemotherapeutic target for PCM.

ACKNOWLEDGMENTS

This work was supported by a grant from FAPESP (99/04126-0). Vicente P. Martins was a recipient of a fellowship from CAPES (DS 103/00). Sérgio A. Uyemura, Carlos Curti, Sergio C. Oliveira, and Gustavo H. Goldman are fellows from CNPq. Frederico M. Soriani and Taisa Magnani Dinamarco were recipients of fellowships from FAPESP.

We thank Márcia Eliana da Silva Ferreira and Marcela Savoldi for assisting with real-time PCR experiments, Yara Maria Lucisano Valim for allowing the use of the microscope in her laboratory, and João J. Franco and Nancy M. F. Rodrigues for providing technical support.

REFERENCES

1. **Bandeira, S. C., and M. P. Nóbrega.** 2008. Characterization of *Paracoccidioides brasiliensis* COX9, COX12, and COX16 respiratory genes. Mycol. Res. **112:**1414–1420.
2. **Barelle, C. J., et al.** 2006. Niche-specific regulation of central metabolic pathways in a fungal pathogen. Cell. Microbiol. **8:**961–971.
3. **Bendtsen, J. D., H. Nielsen, G. von Heijne, and S. Brunak.** 2004. Improved prediction of signal peptides: SignalP 3.0. J. Mol. Biol. **340:**783–795.
4. **Borecky, J., and A. E. Vercesi.** 2005. Plant uncoupling mitochondrial protein and alternative oxidase: energy metabolism and stress. Biosci. Rep. **25:**271–286.
5. **Brummer, E., E. Castaneda, and A. Restrepo.** 1993. Paracoccidioidomycosis: an update. Clin. Microbiol. Rev. **6:**89–117.
6. **Brummer, E., L. H. Hanson, A. Restrepo, and D. A. Stevens.** 1989. Intracellular multiplication of *Paracoccidioides brasiliensis* in macrophages: killing and restriction of multiplication by activated macrophages. Infect. Immun. **57:**2289–2294.
7. **Cardoso., M. A. J. H. Tambor, and F. G. Nobrega.** 2007. The mitochondrial genome from the thermal dimorphic fungus *Paracoccidioides brasiliensis*. Yeast **24:**607–616.
8. **Chance, B., and G. R. Williams.** 1956. The respiratory chain and oxidative phosphorylation. Adv. Enzymol. Relat. Subj. Biochem. **17:**65–134.
9. **Derengowski, L. S., et al.** 2008. Upregulation of glyoxylate cycle genes upon *Paracoccidioides brasiliensis* internalization by murine macrophages and in vitro nutritional stress condition. Med. Mycol. **46:**125–134.
10. **Dinamarco, T. M., et al.** 2010. The roles played by *Aspergillus nidulans* apoptosis-inducing factor (AIF)-like mitochondrial oxidoreductase (AifA) and NADH-ubiquinone oxidoreductases (NdeA-B and NdiA) in farnesol resistance. Fungal Genet. Biol. **47:**1055–1069.
11. **Felipe, M. S., et al.** 2005. Transcriptional profiles of the human pathogenic fungus *Paracoccidioides brasiliensis* in mycelium and yeast cells. J. Biol. Chem. **280:**24706–24714.
12. **Ferreira, M. E., et al.** 2006. Transcriptome analysis and molecular studies on sulfur metabolism in the human pathogenic fungus *Paracoccidioides brasiliensis*. Mol. Genet. Genomics **276:**450–463.
13. **Finlay, B. B., and S. Falkow.** 1997. Common themes in microbial pathogenicity revisited. Microbiol. Mol. Biol. Rev. **61:**136–169.
14. **Garcia, A. M., et al.** 2010. Gene expression analysis of *Paracoccidioides brasiliensis* transition from conidium to yeast cell. Med. Mycol. **48:**147–154.
15. **Gessler, N. N., A. A. Aver'yanov, and T. A. Belozerskaya.** 2007. Reactive oxygen species in regulation of fungal development. Biochemistry **72:**1091–1109.
16. **Gius, D., D. Mattson, C. M. Bradbury, D. K. Smart, and D. R. Spitz.** 2004. Thermal stress and the disruption of redox-sensitive signalling and transcription factor activation: possible role in radiosensitization. Int. J. Hyperthermia **20:**213–223.
17. **Goldman, G. H., et al.** 2003. Expressed sequence tag analysis of the human pathogen *Paracoccidioides brasiliensis* yeast phase: identification of putative homologues of *Candida albicans* virulence and pathogenicity genes. Eukaryot. Cell **2:**34–48.
18. **Gornall, A. G., C. J. Bardawill, and M. M. David.** 1949. Determination of serum proteins by means of the biuret reaction. J. Biol. Chem. **177:**751–766.
19. **Graham, J. E., and J. E. Clark-Curtiss.** 1999. Identification of *Mycobacterium tuberculosis* RNAs synthesized in response to phagocytosis by human macrophages by selective capture of transcribed sequences (SCOTS). Proc. Natl. Acad. Sci. U. S. A. **96:**11554–11559.
20. **Harman, D.** 1956. Aging: a theory based on free radical and radiation chemistry. J. Gerontol. **11:**298–300.
21. **Harman, D.** 1981. The aging process. Proc. Natl. Acad. Sci. U. S. A. **78:**7124–7128.
22. **Harman, D.** 1998. Aging and oxidative stress. J. Int. Fed. Clin. Chem. **10:**24–27.
23. **Helmerhorst, E. J., M. P. Murphy, R. F. Troxler, and F. G. Oppenheim.** 2002. Characterization of the mitochondrial respiratory pathways in *Candida albicans*. Biochim. Biophys. Acta **1556:**73–80.
24. **Huh, W. K., and S. O. Kang.** 2001. Characterization of the gene family encoding alternative oxidase from *Candida albicans*. Biochem. J. **356:**595–604.
25. **Jarmuszkiewicz, W., M. Behrendt, R. Navet, and F. E. Sluse.** 2002. Uncoupling protein and alternative oxidase of *Dictyostelium discoideum*: occurrence, properties and protein expression during vegetative life and starvation-induced early development. FEBS Lett. **532:**459–464.
26. **Jezek, P., and L. Hlavata.** 2005. Mitochondria in homeostasis of reactive oxygen species in cell, tissues, and organism. Int. J. Biochem. Cell Biol. **37:**2478–2503.
27. **Johnson, C. H., J. T. Prigge, A. D. Warren, and J. E. McEwen.** 2003. Characterization of an alternative oxidase activity of *Histoplasma capsulatum*. Yeast **20:**381–388.
28. **Joseph-Horne, T., D. W. Hollomon, and P. M. Wood.** 2001. Fungal respiration: a fusion of standard and alternative components. Biochim. Biophys. Acta **1504:**179–195.
29. **Kerscher, S. J.** 2000. Diversity and origin of alternative NADH:ubiquinone oxidoreductases. Biochim. Biophys. Acta **1459:**274–283.
30. **Kyte, J., and R. F. Doolittle.** 1982. A simple method for displaying the hydropathic character of a protein. J. Mol. Biol. **157:**105–132.
31. **Laemmli, U. K.** 1970. Cleavage of structural proteins during the assembly of the head of bacteriophage T4. Nature **227:**680–685.
32. **Lorenz, M. C., and G. R. Fink.** 2001. The glyoxylate cycle is required for fungal virulence. Nature **412:**83–86.
33. **Lorenz, M. C., and G. R. Fink.** 2002. Life and death in a macrophage: role of the glyoxylate cycle in virulence. Eukaryot. Cell **1:**657–662.
34. **Magnani, T., et al.** 2008. Silencing of mitochondrial alternative oxidase gene of *Aspergillus fumigatus* enhances reactive oxygen species production and killing of the fungus by macrophages. J. Bioenerg. Biomembr. **40:**631–636.
35. **Magnani, T., et al.** 2007. Cloning and functional expression of the mitochondrial alternative oxidase of *Aspergillus fumigatus* and its induction by oxidative stress. FEMS Microbiol. Lett. **271:**230–238.
36. **Malavazi, I., et al.** 2009. Phenotypic analysis of genes whose mRNA accumulation is dependent on calcineurin in *Aspergillus fumigatus*. Fungal Genet. Biol. **46:**791–802.
37. **Maresca, B., et al.** 1981. Role of cysteine in regulating morphogenesis and mitochondrial activity in the dimorphic fungus *Histoplasma capsulatum*. Proc. Natl. Acad. Sci. U. S. A. **78:**4596–4600.
38. **Maresca, B., A. M. Lambowitz, G. Kobayashi, and G. Medoff.** 1979. Respiration in the yeast and mycelial phase of *Histoplasma capsulatum*. J. Bacteriol. **138:**647–649.
39. **Marques, E. R., et al.** 2004. Identification of genes preferentially expressed

in the pathogenic yeast phase of *Paracoccidioides brasiliensis*, using suppression subtraction hybridization and differential macroarray analysis. Mol. Genet. Genomics **271:**667–677.
40. **Martins, V. P., et al.** 2008. Mitochondrial function in the yeast form of the pathogenic fungus *Paracoccidioides brasiliensis*. J. Bioenerg. Biomembr. **40:** 297–305.
41. **Mathy, G., et al.** 2006. *Saccharomyces cerevisiae* mitoproteome plasticity in response to recombinant alternative ubiquinol oxidase. J. Proteome Res. **5:**339–348.
42. **Medoff, G., A. Painter, and G. S. Kobayashi.** 1987. Mycelial- to yeast-phase transitions of the dimorphic fungi *Blastomyces dermatitidis* and *Paracoccidioides brasiliensis*. J. Bacteriol. **169:**4055–4060.
43. **Medoff, G., et al.** 1986. Irreversible block of the mycelial-to-yeast phase transition of *Histoplasma capsulatum*. Science **231:**476–479.
44. **Moore, A. L., A. L. Umbach, and J. N. Siedow.** 1995. Structure-function relationships of the alternative oxidase of plant mitochondria: a model of the active site. J. Bioenerg. Biomembr. **27:**367–377.
45. **Moreira, S. F., et al.** 2004. Monofunctional catalase P of *Paracoccidioides brasiliensis*: identification, characterization, molecular cloning and expression analysis. Yeast **21:**173–182.
46. **Nemecek, J. C., M. Wüthrich, and B. S. Klein.** 2006. Global control of dimorphism and virulence in fungi. Science **312:**583–588.
47. **Nihei, C., et al.** 2003. Purification of active recombinant trypanosome alternative oxidase. FEBS Lett. **538:**35–40.
48. **Nunes, L. R., et al.** 2005. Transcriptome analysis of *Paracoccidioides brasiliensis* cells undergoing mycelium-to-yeast transition. Eukaryot. Cell **4:**2115–2128.
49. **Ohtsuka, Y., N. Yabunaka, H. Fujisawa, I. Watanabe, and Y. Agishi.** 1994. Effect of thermal stress on glutathione metabolism in human erythrocytes. Eur. J. Appl. Physiol. Occup. Physiol. **68:**87–91.
50. **Ramos-E-Silva, M., and E. Saraiva-Ldo.** 2008. Paracoccidioidomycosis. Dermatol. Clin. **26:**257–269.
51. **Rappleye, C. A., and W. E. Goldman.** 2006. Defining virulence genes in the dimorphic fungi. Annu. Rev. Microbiol. **60:**281–303.
52. **Restrepo, A.** 1985. The ecology of *Paracoccidioides brasiliensis*: a puzzle still unsolved. Sabouraudia **23:**323–334.
53. **Restrepo, A., and B. E. Jiménez.** 1980. Growth of *Paracoccidioides brasiliensis* yeast phase in a chemically defined culture medium. J. Clin. Microbiol. **12:**279–281.
54. **Restrepo, A., J. G. McEwen, and E. Castaneda.** 2001. The habitat of *Paracoccidioides brasiliensis*: how far from solving the riddle? Med. Mycol. **39:** 233–241.
55. **Roberts, C. W., et al.** 2004. Evidence for mitochondrial-derived alternative oxidase in the apicomplexan parasite *Cryptosporidium parvum*: a potential anti-microbial agent target. Int. J. Parasitol. **34:**297–308.
56. **Ruy, F., A. E. Vercesi, and A. J. Kowaltowski.** 2006. Inhibition of specific electron transport pathways leads to oxidative stress and decreased *Candida albicans* proliferation. J. Bioenerg. Biomembr. **38:**129–135.
57. **Sacco, M., et al.** 1983. Sulfhydryl induced respiratory "Shunt" pathways and their role in morphogenesis in the fungus, *Histoplasma capsulatum*. J. Biol. Chem. **258:**8223–8230.
57a. **Sambrook, J., E. F. Fritsch, and T. Maniatis.** 1989. Molecular cloning: a laboratory manual, 2nd ed. Cold Spring Harbor Laboratory Press, Cold Spring Harbor, NY.
58. **San-Blas, F., G. San-Blas, and F. Gil.** 1994. Production and regeneration of protoplasts from the Y-phase of the human pathogenic fungus *Paracoccidioides brasiliensis*. J. Med. Vet. Mycol. **32:**381–388.
59. **San-Blas, G., G. Nino-Vega, and T. Iturriaga.** 2002. *Paracoccidioides brasiliensis* and paracoccidioidomycosis: molecular approaches to morphogenesis, diagnosis, epidemiology, taxonomy and genetics. Med. Mycol. **40:**225–242.
60. **Scandalios, J. G.** 2005. Oxidative stress: molecular perception and transduction of signals triggering antioxidant gene defenses. Braz. J. Med. Biol. Res. **38:**995–1014.
61. **Schiestl, R. H., and R. D. Gietz.** 1989. High efficiency transformation of intact yeast cells using single stranded nucleic acids as a carrier. Curr. Genet. **16:**339–346.
62. **Schnappinger, D., et al.** 2003. Transcriptional adaptation of *Mycobacterium tuberculosis* within macrophages: insights into the phagosomal environment. J. Exp. Med. **198:**693–704.
63. **Scott, B., and C. J. Eaton.** 2008. Role of reactive oxygen species in fungal cellular differentiations. Curr. Opin. Microbiol. **11:**488–493.
64. **Semighini, C. P., Z. P. de Camargo, R. Puccia, M. H. Goldman, and G. H. Goldman.** 2002. Molecular identification of *Paracoccidioides brasiliensis* by 5′ nuclease assay. Diagn. Microbiol. Infect. Dis. **44:**383–386.
65. **Siedow, J. N., and A. L. Umbach.** 1995. Plant mitochondrial electron transfer and molecular biology. Plant Cell **7:**821–831.
66. **Siedow, J. N., and A. L. Umbach.** 2000. Plant mitochondrial electron transfer and molecular biology. Biochim. Biophys. Acta **1459:**432–439.
67. **Soriani, F. M., et al.** 2005. A PMR1-like calcium ATPase of *Aspergillus fumigatus*: cloning, identification and functional expression in *S. cerevisiae*. Yeast **22:**813–824.
68. **Soriani, F. M., et al.** 2009. Functional characterization of the *Aspergillus nidulans* methionine sulfoxide reductases (msrA and msrB). Fungal Genet. Biol. **46:**410–417.
69. **Suzuki, T., et al.** 2005. Alternative oxidase (AOX) genes of African trypanosomes: phylogeny and evolution of AOX and plastid terminal oxidase families. J. Eukaryot. Microbiol. **52:**374–381.
70. **Tavares, A. H., et al.** 2007. Early transcriptional response of *Paracoccidioides brasiliensis* upon internalization by murine macrophages. Microbes Infect. **9:**583–590.
71. **Tischner, R., E. Planchet, and W. M. Kaiser.** 2004. Mitochondrial electron transport as a source for nitric oxide in the unicellular green alga *Chlorella sorokiniana*. FEBS Lett. **576:**151–155.
72. **Tudella, V. G., C. Curti, F. M. Soriani, A. C. Santos, and S. A. Uyemura.** 2004. In situ evidence of an alternative oxidase and an uncoupling protein in the respiratory chain of *Aspergillus fumigatus*. Int. J. Biochem. Cell Biol. **36:**162–172.
73. **Vacca, R. A., et al.** 2004. Production of reactive oxygen species, alteration of cytosolic ascorbate peroxidase, and impairment of mitochondrial metabolism are early events in heat shock-induced programmed cell death in tobacco Bright-Yellow 2 cells. Plant Physiol. **134:**1100–1112.
74. **Vanlerberghe, G. C., and L. McIntosh.** 1997. Alternative oxidase: from gene to function. Annu. Rev. Plant Physiol. Plant Mol. Biol. **48:**703–734.
75. **Veiga, A., J. D. Arrabaca, and M. C. Loureiro-Dias.** 2003. Cyanide-resistant respiration, a very frequent metabolic pathway in yeasts. FEMS Yeast Res. **3:**239–245.